

# Transform-limited spectral compression due to self-phase modulation in fibers

Brian R. Washburn

*School of Physics, Georgia Institute of Technology, Atlanta, Georgia 30332*

John A. Buck and Stephen E. Ralph

*School of Electrical and Computer Engineering, Georgia Institute of Technology, Atlanta, Georgia 30332*

Received December 7, 1999

We demonstrate near-transform-limited pulse generation through spectral compression arising from nonlinear propagation of negatively chirped pulses in optical fiber. The output pulse intensity and phase were quantified by use of second-harmonic generation frequency-resolved optical gating. Spectral compression from 8.4 to 2.4 nm was obtained. Furthermore, the phase of the spectrally compressed pulse was found to be constant over the spectral and temporal envelopes, which is indicative of a transform-limited pulse. Good agreement was found between the experimental results and numerical pulse-propagation studies. © 2000 Optical Society of America

OCIS codes: 060.4370, 320.1590, 320.7100, 320.5540, 320.2250.

Self-phase modulation (SPM) in optical fiber is ordinarily associated with spectral broadening of an ultrashort optical pulse. However, for appropriate initial conditions of the input pulse, SPM can result in significant spectral compression. Indeed, SPM causes spectral compression or broadening depending on the initial frequency modulation (chirp) of the pulse electric field,  $E(t)$ . Specifically, a negatively chirped pulse is compressed by the effects of SPM.<sup>1</sup> We use the term spectral compression to stress that for a negatively chirped pulse SPM transfers pulse energy to spectral components that are closer to the center wavelength without energy loss. Applications of spectral compression include the low-loss generation of ~1-ps transform-limited pulses from ~100-fs pulses and the use of these spectrally compressed pulses in fiber links.<sup>2,3</sup> Although it has been suggested that SPM can be used to generate a longer-duration transform-limited pulse<sup>4</sup> from a short pulse source, to date researchers have not reported on the phase behavior of the compressed pulse. We have quantified the transform-limited nature of the spectrally compressed pulses by assessing the pulse intensity and phase. An initially negatively chirped pulse is characterized before and after propagation through single-mode fiber (SMF) in the normal group-velocity dispersion region. We demonstrate a spectral compression ratio of 4 to 1, with a resultant phase that is constant over the pulse envelope. Furthermore, our numerical investigation is in good agreement with the experimental observations.

The effect of SPM is to redistribute the pulse energy to different spectral components. The origin of this redistribution is the intensity-dependent nonlinear phase shift  $\varphi_{\text{NL}}(t) \propto |E(t)|^2$ . The result of this nonlinear phase shift, in silica, is a frequency downshift ( $\delta\omega < 0$ ) in the leading edge of the pulse and an upshift ( $\delta\omega > 0$ ) in the trailing edge.<sup>5</sup> Specifically,

$$\delta\omega(t) = -\frac{\partial\varphi_{\text{NL}}}{\partial t} \propto -\frac{\partial}{\partial t}|E(t)|^2. \quad (1)$$

Thus the effect of SPM is dependent on the sign of the initial chirp. Negatively chirped pulses, where the long and the short wavelengths are in the trailing and the leading edges, respectively, are spectrally compressed, since both the long and the short wavelengths are shifted toward the center wavelength ( $\lambda_0$ ). Spectral broadening occurs for pulses that are positively chirped or transform limited. It is therefore important to know the initial chirp if the effects of SPM are to be predicted. We employ second-harmonic-generation frequency-resolved optical gating<sup>6</sup> to determine the pulse intensity and phase.

The initial sech<sup>2</sup> pulse was generated by a mode-locked Ti:sapphire laser at  $\lambda_0 = 810$  nm. The pulse duration was 110 fs (FWHM), with a time-bandwidth product of 0.34. We created the negative chirp by first propagating the pulse through a double-pass SF-10 prism-pair geometry<sup>7</sup> [Fig. 1(a)]. The negatively chirped pulse was then coupled into 0.5 m of SMF that served as the source of SPM. An amplitude and phase assessment was made by use of frequency-resolved optical gating (FROG) on (i) the initial laser pulse (location ①), (ii) the negatively chirped pulse (location ②), and (iii) the spectrally compressed pulse (location ③).

We characterized the negative chirp before the fiber and determined that for  $L_p = 3$  m the pulse was strongly chirped with a temporal FWHM of 665 fs. The spectral phase was retrieved by the FROG algorithm and fitted to a Taylor series expansion including quadratic ( $\varphi_2 \equiv d^2\varphi/d\omega^2|_{\omega_0}$ ) and cubic ( $\varphi_3 \equiv d^3\varphi/d\omega^3|_{\omega_0}$ ) phase-distortion terms. The rms error  $G$  between the normalized experimental spectrogram and the retrieved FROG spectrogram was very small, typically  $G = 0.0022$ . Although the sign of the observed chirp is ambiguous for SHG FROG, we also observed the expected linear dependence of the magnitude of the linear chirp on the prism separation. This dependence, together with the observation of enhanced compression with increasing prism separation,

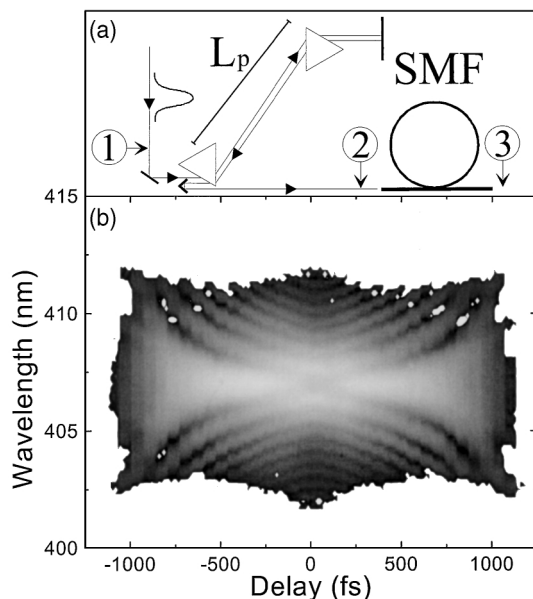


Fig. 1. (a) Experimental spectral compression setup, showing the prism separation of  $L_p = 3$  m. Pulse characterization was performed at locations ①, ②, and ③. (b) Measured FROG spectrogram after the prism pair and the SMF (location ③). Spectral compression increases near-zero delay resulting from larger SPM at higher intensities. Average power in the fiber was 70 mW (8400-W peak power).

confirms the existence of the expected negative chirp. The phase distortion measured after the prism pair was  $\varphi_2 = -30,600 \text{ fs}^2$  and  $\varphi_3 = -79,100 \text{ fs}^3$ . These values compare well with the calculated phase distortion imposed by the isolated prism-pair geometry,<sup>7</sup> which is  $\varphi_{2,\text{cal}} = -45,000 \text{ fs}^2$  and  $\varphi_{3,\text{cal}} = -102,000 \text{ fs}^3$ . The smaller measured phase distortion results mostly from the positive  $\varphi_2$  and  $\varphi_3$  of the experimental optics. The near-transform-limited initial pulse exhibited a small phase distortion, typically  $\varphi_2 = +120 \text{ fs}^2$  and  $\varphi_3 = +2000 \text{ fs}^3$ .

The negatively chirped pulse was then spectrally compressed in 0.5 m of SMF (location ③; Fig. 1). The pulse-power dependence of the compression was investigated by use of both FROG and separate spectral measurements. The average power at the SMF output was varied from 5 to 70 mW by attenuation at the fiber input. A FROG spectrogram for 70-mW average power is shown in Fig. 1(b). The SHG spectral width can be seen to narrow near-zero delay resulting from the enhanced SPM at higher intensities. The fundamental spectral FWHM (time integrated) was 2.5 nm, and the temporal FWHM was 946 fs ( $G = 0.007$ ). We note that the retrieved phase revealed significant positive chirp. Thus at 70-mW average power the total SPM was in excess of that needed to compensate for the initial negative chirp. At 40 mW the resultant phase distortion was near minimum, producing a near-transform-limited pulse. Indeed, significant spectral compression occurred for powers greater than 25 mW (Fig. 2). Spectra at these powers also show structure and a slight asymmetry, which we associate with the cubic phase distortion produced by the prism pair.

The retrieved spectrum, temporal intensity, and corresponding phase are shown in Fig. 3 for 40-mW average power. The initial spectral FWHM of 8.4 nm is compressed to 2.4 nm, and the temporal FWHM broadens from 110 to 600 fs. Importantly, the phase is constant over the FWHM of the spectrum, which is indicative of a transform-limited pulse. We note that the temporal FWHM of the negatively chirped pulse (measured at location ②) remains essentially unchanged after spectral compression, although the

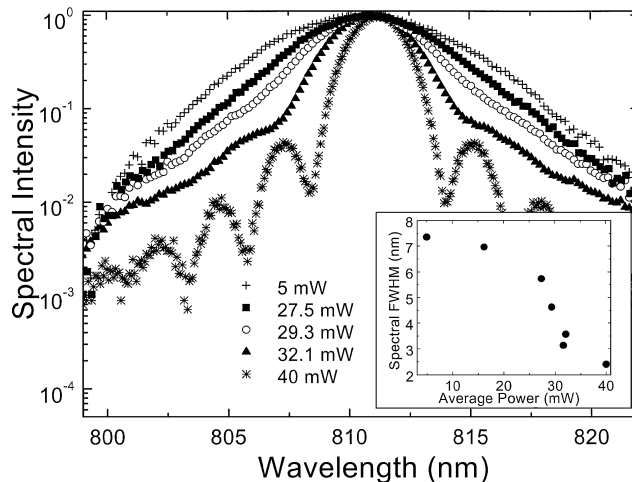


Fig. 2. Observed spectra measured at location ③ for increasing average power. Inset, spectral FWHM versus average power.

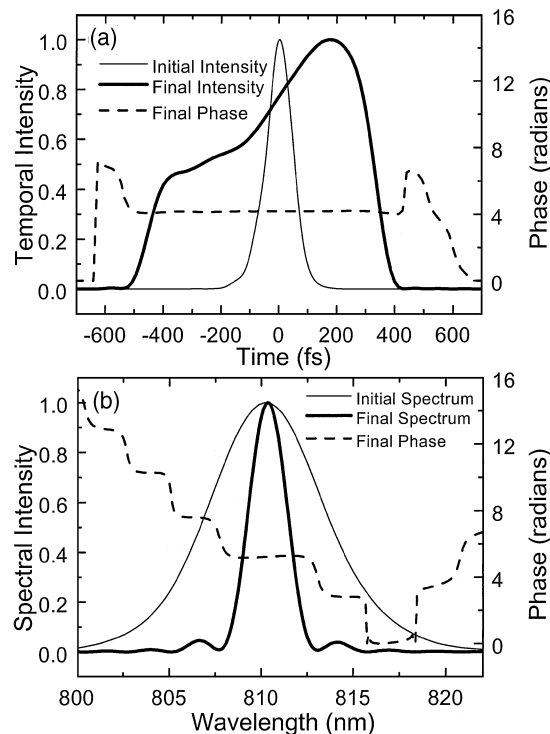


Fig. 3. Retrieved intensity and phase: (a) temporal and (b) spectral for an average power of 40 mW measured at location ③ (FROG error of  $G = 0.0027$ ). The phase over the temporal and spectral FWHM is free of significant distortion. The initial  $\text{sech}^2$  pulse temporal and spectral intensity (location ①) is shown for comparison (thin curves).

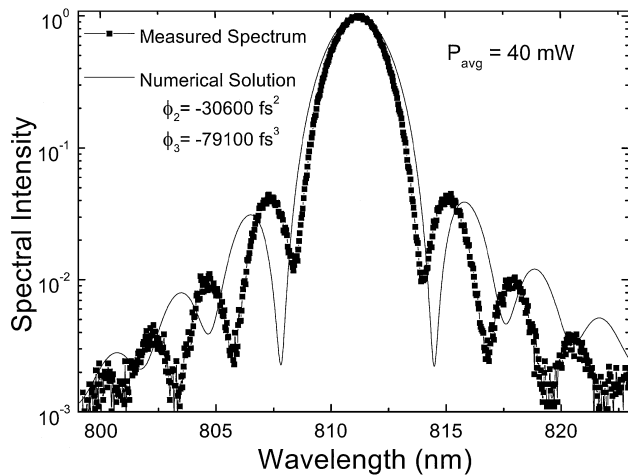


Fig. 4. Numerical solution where  $E_p(\omega)$  was calculated with the measured phase distortions  $\varphi_2$  and  $\varphi_3$ . The experimentally measured spectrum is shown to be very similar to it. Note that the measured spectrum is nearly identical to the FROG retrieved spectrum of Fig. 3.

pulse shape becomes somewhat asymmetric owing to the residual phase distortion.

The propagation of an ultrashort pulse through SMF is theoretically described by the nonlinear Schrödinger equation (NLSE).<sup>5</sup> The NLSE accounts for the effects of material absorption, group-velocity dispersion, and optical nonlinearity owing to propagation through the fiber. To verify the experimental results we solved the NLSE for propagation through the prism pair and the SMF, using the split-step Fourier method.<sup>5</sup> The resultant electric field from the prism pair  $E_p(\omega)$  was first calculated with

$$E_p(\omega) = \mathcal{F}[E_0 \operatorname{sech}(t/t_0)] \exp[i(\varphi_2 \omega^2/2 + \varphi_3 \omega^3/6)], \quad (2)$$

where  $E_0 \operatorname{sech}(t/t_0)$  is the initial electric field and  $\mathcal{F}$  denotes the Fourier transform. The experimental values of  $\varphi_2$  and  $\varphi_3$  were used in Eq. (2). The inverse Fourier transform was then used to generate  $E_p(t)$ , which was used as the input for the split-step Fourier method. The calculated intensity  $|E_p(t)|^2$  compares well with the experimental intensity at location ②. The NLSE was solved for pulse propagation through 0.5 m of SMF with a spatial step size of 100  $\mu\text{m}$ . The NLSE included quadratic ( $\beta_2$ ) and cubic ( $\beta_3$ ) group-velocity dispersion calculated from the manufacturer's dispersion parameters.<sup>8</sup> The effect of third-order nonlinearity (SPM) was contained in the nonlinear refractive index ( $n_2 = 3.2 \times 10^{-20} \text{ m}^2/\text{W}$ ); higher-order

nonlinearities and material absorption were assumed to be negligible owing to the short length of fiber. We chose the spatial step size to ensure conservation of pulse energy. The final pulse energy was within  $5 \times 10^{-5}\%$  of the initial energy for the chosen spatial step. A comparison of the calculated and the measured spectra for an average power of 40 mW (4800-W peak power) is shown in Fig. 4. Importantly, the directly measured spectrum of Fig. 4 is nearly identical to the retrieved spectrum of Fig. 3. The spectral FWHM calculated by the split-step Fourier method was 2.89 nm, compared with the measured FWHM of 2.4 nm. The numerical phase compared well with the retrieved phase and was also constant over the pulse FWHM. Note that, if  $E_p(\omega)$  is calculated with  $\varphi_{2,\text{cal}}$  and  $\varphi_{3,\text{cal}}$  instead, the numerical spectrum does not compare well with the experimental spectrum. This illustrates the sensitivity of the spectral compression to the degree of initial negative chirp. Our central results are not altered by the dispersion of the short fiber. However, the compression performance is ultimately limited by the dispersion and its interplay with SPM.

In conclusion, we have demonstrated the ability to spectrally compress ultrashort pulses with commensurate temporal broadening to produce longer pulses with constant phase over the field envelope. This ability is clearly illustrated by the results from the spectral and the FROG measurements. The numerical solution to the NLSE is in good agreement with our experiment results.

S. E. Ralph's e-mail address is stephen.ralph@ece.gatech.edu.

## References

1. S. A. Planas, N. L. Pires Mansur, C. H. Brito Cruz, and H. L. Fragnito, *Opt. Lett.* **18**, 699 (1993).
2. S. T. Cundiff, B. C. Collings, L. Boivin, M. C. Nuss, K. Bergman, W. H. Knox, and S. G. Evangelides, Jr., *J. Lightwave Technol.* **17**, 811 (1999).
3. S. Shen, C. Chang, H. P. Sardesai, V. Binjrajka, and A. M. Weiner, *J. Lightwave Technol.* **17**, 452 (1999).
4. M. Oberthaler and R. A. Höpfel, *Appl. Phys. Lett.* **63**, 1017 (1993).
5. G. P. Agrawal, *Nonlinear Fiber Optics* (Academic, San Diego, Calif., 1995).
6. K. W. DeLong, R. Trebino, J. Hunter, and W. E. White, *J. Opt. Soc. Am. B* **11**, 2206 (1994).
7. R. L. Fork, O. E. Martinez, and J. P. Gordon, *Opt. Lett.* **9**, 150 (1984).
8. SpecTran Specialty Optics Co., fiber number CFO4247-04. The dispersion parameters are  $D = -113 \text{ ps}/(\text{km}/\text{nm})$  and  $dD/d\lambda = 0.4 \text{ ps}/(\text{km}\cdot\text{nm}^2)$ .